Bicarbonate Cotransporter NBCn1 in the Kidney Medullary Thick Ascending Limb Cell Line is Upregulated under Acidic Conditions and Enhances Ammonium Transport

Soojung Lee, *Emory University*
Hye Jeong Lee, *Emory University*
Han Soo Yang, *Emory University*
Ian M. Thornell, *University of Alabama at Birmingham*
Mark O. Bevensee, *University of Alabama at Birmingham*
Inyeong Choi, *Emory University*

Journal Title: Experimental Physiology
Volume: Volume 95, Number 9
Publisher: Wiley: 12 months | 2010-09, Pages 926-937
Type of Work: Article | Final Publisher PDF
Publisher DOI: 10.1113/expphysiol.2010.053967
Permanent URL: http://pid.emory.edu/ark:/25593/ffc7f

Final published version: http://ep.physoc.org/content/95/9/926.long

Exp Physiol 95.9 pp 926–937

Experimental Physiology – *Research Paper*

Sodium–bicarbonate cotransporter NBCn1 in the kidney medullary thick ascending limb cell line is upregulated under acidic conditions and enhances ammonium transport

Soojung Lee[1], Hye Jeong Lee[1], Han Soo Yang[1], Ian M. Thornell[2], Mark O. Bevensee[2] and Inyeong Choi[1]

[1]*Department of Physiology, Emory University School of Medicine, Atlanta, GA 30322, USA*
[2]*Department of Physiology and Biophysics, University of Alabama at Birmingham, Birmingham, AL 35294, USA*

In this study, we examined the effect of bicarbonate transporters on ammonium/ammonia uptake in the medullary thick ascending limb cell line ST-1. Cells were treated with 1 mM ouabain and 0.2 mM bumetanide to minimize carrier-mediated NH_4^+ transport, and the intracellular accumulation of ^{14}C-methylammonium/methylammonia (^{14}C-MA) was determined. In CO_2/HCO_3^--free solution, cells at normal pH briefly accumulated ^{14}C-MA over 7 min and reached a plateau. In CO_2/HCO_3^- solution, however, cells markedly accumulated ^{14}C-MA over the experimental period of 30 min. This CO_2/HCO_3^--dependent accumulation was reduced by the bicarbonate transporter blocker, 4,4′-diisothiocyanatostilbene-2,2′-disulfonate (DIDS; 0.5 mM). Replacing Cl^- with gluconate reduced the accumulation, but the reduction was more substantial in the presence of DIDS. Incubation of cells at pH 6.8 (adjusted with $NaHCO_3$ in 5% CO_2) for 24 h lowered the mean steady-state intracellular pH to 6.96, significantly lower than 7.28 for control cells. The presence of DIDS reduced ^{14}C-MA accumulation in control conditions but had no effect after acidic incubation. Immunoblotting showed that NBCn1 was upregulated after acidic incubation and in NH_4Cl-containing media. The Cl^-–HCO_3^- exchanger AE2 was present, but its expression remained unaffected by acidic incubation. Expressed in *Xenopus* oocytes, NBCn1 increased carrier-mediated ^{14}C-MA transport, which was abolished by replacing Na^+. Two-electrode voltage clamp of oocytes exhibited negligible current after NH_4Cl application. These results suggest that DIDS-sensitive HCO_3^- extrusion normally governs NH_4^+/NH_3 uptake in the medullary thick ascending limb cells. We propose that, in acidic conditions, DIDS-sensitive HCO_3^- extrusion is inactivated, while NBCn1 is upregulated to stimulate NH_4^+ transport.

(Received 14 May 2010; accepted after revision 22 June 2010; first published online 30 June 2010)
Corresponding author I. Choi: Department of Physiology, Emory University School of Medicine, 615 Whitehead Research Building, Atlanta, GA 30322, USA. Email: ichoi@emory.edu

One of the major tasks of the kidney is to maintain acid–base homeostasis in the body. The kidney regulates blood pH by reclaiming filtered acid or base equivalents or by releasing them into urine. The major acid–base component that the kidney regulates is HCO_3^-. In the medullary thick ascending limb (MTAL), where 10–15% of filtered HCO_3^- is reclaimed, HCO_3^- absorption is initiated by H^+ secretion into the lumen via the apical Na^+–H^+ exchanger, NHE3 (Good & Watts, 1996), accompanied by HCO_3^- exit to the medullary interstitium. The basolateral HCO_3^- exit is probably mediated by the Cl^-–HCO_3^- exchanger, AE2 (Brosius *et al.* 1995; Sun, 1998). However, Na^+–HCO_3^- transporters (Kikeri *et al.* 1990; Vorum *et al.* 2000; Xu *et al.* 2003) and K^+–Cl^- cotransporter-mediated HCO_3^- exit (Bourgeois *et al.* 2002) have also been reported.

The MTAL also handles NH_4^+/NH_3 that serve as major non-bicarbonate buffer components in the kidney (for review, see Weiner & Hamm, 2007). The ammonium ion, which is produced in the proximal tubules and secreted to the lumen, is absorbed via the apical Na^+–K^+–$2Cl^-$ cotransporter, NKCC2 (Kinne *et al.* 1986), and dissociates intracellularly into NH_3 and H^+. Ammonia then moves

S. Lee and H. J. Lee contributed equally to this work.

DOI: 10.1113/expphysiol.2010.053967

to the medullary interstitium and reassociates with H^+ to form NH_4^+. This process provides a concentration gradient of NH_3 across the cells, which ultimately enables NH_3 to diffuse into the collecting ducts for urinary excretion or to the renal vein for recycling. The blood type Rh glycoprotein family proteins are mammalian ammonium transporters (Marini *et al.* 2000; Liu *et al.* 2000, 2001) and are found in the proximal tubules and collecting ducts, but not in the MTAL (Verlander *et al.* 2003).

The HCO_3^- and NH_4^+ movements are associated with each other in many nephron segments, including the MTAL (Good, 1994; Kraut & Kurtz, 2005; Wagner, 2007). The physiological coupling between these two ion transport processes is particularly evident during cellular and systemic pH changes. The absorptive capacity for HCO_3^- and NH_4^+ is increased in response to chronic metabolic acidosis, and this change typically involves up- or downregulation of membrane proteins responsible for transporting acid/base equivalents (for review, see Good, 1994; Wagner, 2007). Among these proteins, NBCn1 is of particular interest. This transporter normally moves Na^+ and HCO_3^- into the cell, but it is localized to the basolateral membrane of the MTAL. *In vivo* animal studies show a nearly 10-fold increase in NBCn1 protein expression in chronic metabolic acidosis induced by NH_4Cl load (Kwon *et al.* 2002; Odgaard *et al.* 2004). The upregulation of NBCn1 occurs probably to counter H^+ overload caused by an increase in NH_4^+ uptake. Consistent with this compensatory function, NBCn1 in neurons is upregulated in acidic conditions (Park *et al.* 2010).

In this study, we examined the effect of HCO_3^- transporters on NH_4^+/NH_3 uptake in the MTAL cell line ST-1. This cell line is a non-polarized cell and exhibits many features characteristic of MTAL cells (Kone *et al.* 1995; Kone & Higham, 1999). We measured intracellular accumulation of ^{14}C-methylammonium/methylammonia (^{14}C-MA) and evaluated the effects of DIDS, as well as ion replacement, on ^{14}C-MA accumulation. The effect of acidic pH on NH_4^+/NH_3 uptake was evaluated by measuring 14C-MA accumulation after acidic incubation of the cells. The NBCn1 transporter was then expressed in *Xenopus* oocytes and examined for its ability to accumulate ^{14}C-MA and affect pH changes mediated by NH_4^+ transport. Our data suggest that NBCn1 plays dynamic roles in regulating HCO_3^- and NH_4^+ transport in the MTAL cells.

Methods

ST-1 cells

The ST-1 cells (provided by Bruce Kone, University of Florida) were cultured in Dulbecco's modified Eagle's medium supplemented with 10% fetal bovine serum, 50 U ml^{-1} penicillin and 50 μg ml^{-1} streptomycin in a 5% CO_2 air equilibrated 37°C incubator (Kone & Higham, 1999). For ^{14}C-MA accumulation assay, cells were plated on 24-well plates at a density of 0.2–3.5 $\times$ 10^5 cells per well and incubated for 1–4 days. For acidification experiments, cells were plated on six-well plates at a density of 2.2–8.8 $\times$ 10^4 cells per well until cells were >90% confluent. The pH in the medium was adjusted by varying HCO_3^- concentration according to the Henderson–Hasselbalch equation with the solubility coefficient of 0.03 mmol CO_2 mmHg^{-1} and P_{CO_2} of 35.65 mmHg.

Measurements of pH_i in ST-1 cells

Steady-state pH_i was determined according to the protocol of Cooper *et al.* (2009) with a slight modification. Briefly, cells grown on a coverslip (>60% confluent) were loaded with 6.5 μM of 2′,7′-bis(2-carboxyethyl)-5(6)-carboxyfluorescein acetoxymethyl ester (BCECF-AM) for 10 min and then mounted in a closed chamber, RC-30 (Warner Instruments, Hamden, CT, USA), affixed on the stage of a Zeiss Axiovert 135 inverted microscope (Zeiss, Oberkochem, Germany). The microscope was equipped with a Lambda 10–2 filter wheel controller and a multiwavelength filter set (Sutter Instruments, Novato, CA, USA). The dye was alternately excited with 490 and 440 nm light, and the emission light at 535 nm (i.e. I_{490} and I_{440}) was captured. The ratio of I_{490}/I_{440} was calculated after background subtraction. Dye calibration was done using nigericin. Steady-state pH_i in CO_2/HCO_3^- solution was calculated by determining linear least squares analysis over a minimum of 20 s. Data were acquired using Nikon NIS Elements AR 3.0 (Nikon, Melville, NY, USA).

Immunoblotting

Cells were scraped in ice-cold homogenization buffer containing 300 mM mannitol, 5 mM Hepes (pH 7.2), 0.1 mg ml^{-1} phenylmethanesulphonyl fluoride and 1× protease inhibitor cocktail I (Calbiochem, San Diego, CA, USA). Cells were homogenized with a 26 gauge needle and centrifuged at 810*g* for 10 min at 4°C, and supernatants were ultracentrifuged at 100,000*g* for 30 min at 4°C. Membrane pellets were collected and dissolved in PBS, and protein concentration was determined using the Bradford reagents (Sigma-Aldrich, St Louis, MO, USA). The equal amounts of protein samples were separated on a 7.5% SDS polyacrylamide gel and blotted to a polyvinylidene fluoride membrane. The blot was incubated in PBS containing 0.05% Tween 20 and 5% non-fat dry milk for 1 h and then treated with antibodies to rat NBCn1 (Cooper *et al.* 2009) and AE2 (Frische *et al.* 2004). The blot was washed with PBS containing 0.05% Tween 20 and

then incubated with a horseradish peroxidase-conjugated secondary antibody (1:2500 dilution) for 1 h (Millipore, Billerica, MA, USA). The blot was washed and visualized by enhanced chemiluminescence (ECL; GE Healthcare, Chicago, IL, USA). For β-actin, the blot was striped with 62.6 mM Tris–HCl (pH 6.7), 2% SDS and 0.7% β-mercaptoethanol at 50°C for 5 min, and reprobed with the mouse β-actin antibody (Millipore). For quantification, mean pixel intensities of immunoreactive signals were measured by positioning boxes around protein bands using ImageJ image analysis software (NIH, Bethesda, MD, USA). The intensity values for NBCn1 and AE2 were normalized to the intensity value for β-actin after background subtraction.

Accumulation of ^{14}C-MA

Cells grown on a 24-well plate were treated with the assay solution [mM: 140 NaCl, 1 KCl, 2 $CaCl_2$, 1 $MgSO_4$, 2.5 NaH_2PO_4, 5.5 glucose, 10 Hepes (pH 7.4), 1 ouabain and 0.2 bumetanide; 2 ml per well] for 20–30 min, and then incubated in the fresh ^{14}C-MA assay solution containing 0.5 mM CH_3-NH_3Cl and 1 μCi ml^{-1} $^{14}CH_3$-NH_3Cl (ICN, Costa Mesa, CA, USA). For CO_2/HCO_3^--buffered solution, 33 mM $NaHCO_3$ replaced the equimolar concentration of NaCl, and the solution was equilibrated with 5% CO_2 in air for 30 min. For ion replacement experiments, Na^+ was substituted with *N*-methyl-D-glucamine ($NMDG^+$) and Cl^- with gluconate. To block HCO_3^- transporters, 0.5 mM 4,4′-diisothiocyanato-2,2′-disulfonate stilbene (DIDS; Sigma-Aldrich) was included in the ^{14}C-MA assay solution. Experiments were terminated at different time points by washing cells four times with ice-cold non-radioactive assay solution containing 1 mM methylammonium/methylammonia (MA). Cells were solubilized in 2% SDS in 0.1 N NaOH, and the radioactivity was determined using a Packard Tricarb scintillation counter (PerkinElmer, Waltham, MA, USA). Each time point was an independent measurement. The counts (count per minute; c.p.m.) were divided by the mean specific activity of ^{14}C-MA assay solution and presented as pmoles per microgram total protein. For ^{14}C-MA accumulation experiments with oocytes, three to five oocytes were incubated with the ^{14}C-MA assay solution in the absence or presence of 5% CO_2, 25 mM HCO_3^- (pH 7.4) without bumetanide and ouabain.

Expression of NBCn1 in *Xenopus* oocytes

Frogs were purchased from Xenopus Express (Brooksville, FL, USA). A frog was anaesthetized with fresh 0.1% 3-aminobenzoic acid ethyl ester (tricaine, Sigma-Aldrich) in 5 mM Hepes (pH 7.5) for 20 min. The frog was then placed on ice, and surgery was done to collect oocytes. After surgery, the frog was placed in a recovery tank containing 0.1 M NaCl until the animal was fully recovered. Oocytes were washed with Ca^{2+}-free solution containing (mM): 96 NaCl, 2 KCl, 1 $MgCl_2$, 10 Hepes (pH 7.4) five times for 20 min each, and then agitated with 2 mg ml^{-1} type IA collagenase (Sigma-Aldrich) twice for 20 min each. Oocytes without follicles (stage V–VI) were manually sorted and stored in OR3 medium (Chang *et al.* 2008) at 18°C overnight. For cRNA injection, the plasmid containing rat NBCn1-E (Cooper *et al.* 2005) was linearized with *Nhe*I and *in vitro* transcribed using the mMessage/mMachine transcription kit (Ambion, Austin, TX, USA). Injection was done with 46 nl of either NBCn1-E cRNA (25 ng) or sterile water. Oocytes were maintained at 18°C for 3 days. Experiments requiring the use of frogs were conducted under the NIH guidelines for research on animals, and the protocols were approved by the Institutional Animal Care and Use Committee at Emory University and University of Alabama at Birmingham.

Electrophysiology

An oocyte was impaled with current and voltage electrodes filled with 3 M KCl. The electrode resistance was <1.5 MΩ for both. The oocyte was superfused with the recording solution (mM: 80 NaCl, 20 NMDG-Cl, 2 KCl, 1 $MgCl_2$, 1.8 $CaCl_2$ and 5 Hepes, pH 7.5) and clamped at -60 mV using the oocyte clamp OC-725C (Warner). Step voltage commands from -120 to $+40$ mV (100 ms, 20 mV increments) were applied before and ∼1 min after the switch to the recording solution containing 20 mM NH_4Cl. The $NMDG^+$ was replaced with NH_4^+. Current and voltage signals were collected using a Digidata 1322 interface (Molecular Devices, Sunnyvale, CA, USA), and data were acquired and analysed using pClamp 8 (Molecular Devices). Experiments were done at room temperature.

Statistical analysis

Data are reported as means ± S.E.M. For level of significance, a one-way ANOVA with Bonferroni *post hoc* test was used to compare the ratio of NBCn1/β-actin expression at different time points. A two-way ANOVA with Bonferroni *post hoc* test was used to compare ^{14}C-MA accumulation at different time points. Student's unpaired, one-tailed *t* test was used to analyse the following: (1) ^{14}C-MA accumulation and pH_i after acidic incubation; (2) quantification of immunoblot signals; and (3) conductance and zero-current voltage in oocytes. Values of $P < 0.05$ were considered significant. The *n* value refers to the number of independent experiments for ^{14}C-MA accumulation assay and immunoblotting,

and the number of oocytes that were independently prepared from four experiments. Data were analysed using Microsoft Excel and Origin 8.1 software (OriginLab Corp., Northampton, MA, USA).

Results

Accumulation of ^{14}C-MA in ST-1 cells is stimulated by HCO_3^- transporters

To examine whether HCO_3^- transporters affect NH_4^+/NH_3 uptake, we treated cells with the ^{14}C-MA assay solution (pH 7.4) and measured the radioisotope accumulated in cells. Both CH_3-NH_2 diffusion and carrier-mediated CH_3-NH_3^+ transport affect ^{14}C-MA accumulation in the non-polarized ST-1 cells. This complicates our study examining the effect of HCO_3^- transporters on NH_4^+/NH_3 uptake in the cells because HCO_3^- transporters change intracellular pH (pH_i), to which NH_4^+ transporters such as NKCC2 (Gamba & Friedman, 2009) and Na^+, K^+-ATPase (Kaplan, 2002) are sensitive. For this and subsequent experiments, 0.2 mM bumetanide and 1 mM ouabain (Kone & Higham, 1999) were included in the assay solution to minimize carrier-mediated CH_3-NH_3^+ transport. Thus, the ^{14}C-MA accumulation value in our experiments primarily reflects the amount of CH_3-NH_3^+ that is converted from CH_3-NH_2 and trapped in the cell.

Figure 1*A* shows the time course of mean ^{14}C-MA accumulation in the absence of 5% CO_2, 33 mM HCO_3^- (pH 7.4). The accumulation increased over ∼7 min and then reached a plateau, reflecting no net movement of CH_3-NH_3^+/CH_3-NH_2 across the cell membrane. In these conditions, DIDS had negligible effect ($n = 3$; $P > 0.05$; two-way ANOVA with Bonferroni *post hoc* test). In contrast, parallel experiments with sister plates showed that ^{14}C-MA accumulation was greater in the presence of 5% CO_2, 33 mM HCO_3^- (Fig. 1*B*). The dashed line in Fig. 1*B* represents the time course of the accumulation measured in CO_2/HCO_3^--free solution. The CO_2/HCO_3^--dependent ^{14}C-MA accumulation was markedly reduced by 0.5 mM DIDS ($n = 3$; $P < 0.05$; two-way ANOVA with Bonferroni *post hoc* test). The reduction was particularly substantial over 12 min and then less effective afterwards. Thus, at 22 min, ∼37% of the accumulation was inhibited by DIDS.

The above results indicate that DIDS-sensitive HCO_3^- transporters assist in providing H^+ and influence intracellular NH_4^+ trapping. Such a process is expected in an acid-loading transporter that removes HCO_3^- from the cell. The DIDS-sensitive HCO_3^- extrusion in the MTAL is governed by the Cl^-–HCO_3^- exchanger (Quentin *et al.* 2004). To test whether the Cl^-–HCO_3^- exchanger is involved in the process of NH_4^+ trapping in our experiments, we replaced Cl^- in the assay solution with gluconate and measured ^{14}C-MA accumulation over 10–30 min after treatment, during which time the accumulation reached a plateau in CO_2/HCO_3^--free solution. Replacing Cl^- progressively reduced the accumulation over time compared with control

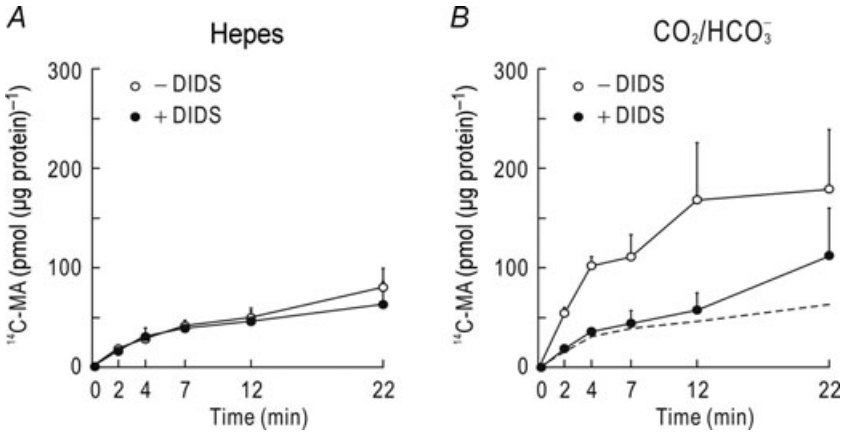

Figure 1. Accumulation of ^{14}C-methylammonium/methylammonia (^{14}C-MA) in cells
A, ^{14}C-MA accumulation in CO_2/HCO_3^--free solution (pH 7.4). Cells grown on a 24-well plate were treated with CO_2/HCO_3^--free ^{14}C-MA assay solution. Cells were then rapidly rinsed with ice-cold wash solution containing unlabelled MA at different time points. The ^{14}C-MA assay solution in this and subsequent experiments with ST-1 cells contained 0.2 mM bumetanide and 1 mM ouabain to minimize carrier-mediated CH_3-NH_3^+ transport. Experiments were done in the presence or absence of 0.5 mM 4,4′-diisothiocyanatostilbene-2,2′-disulfonate (DIDS). The accumulation is presented as pmoles per microgram total protein. Data were averaged from three experiments. *B*, ^{14}C-MA accumulation in CO_2/HCO_3^- solution. The experimental procedure was identical to that in *A* except that the assay solution contained 5% CO_2, 33 mM HCO_3^- (pH 7.4). The dashed line was derived from the line (closed circles) in *A*. Data were averaged from three experiments.

conditions (Fig. 2*A*), consistent with the idea that the absence of external Cl^- decreases HCO_3^- exit and the concomitant H^+ needed to trap ^{14}C-MA. Nonetheless, adding 0.5 mM DIDS to the Cl^--replaced assay solution caused a more profound decrease, comparable to the inhibition by DIDS in Cl^--containing assay solution (Fig. 1*B*). Thus, Cl^- removal partly inhibited CO_2/HCO_3^--dependent ^{14}C-MA accumulation. In the MTAL, DIDS-sensitive HCO_3^- exit can occur via the K^+–Cl^- cotransporter (Bourgeois *et al.* 2002) in addition to the Cl^-–HCO_3^- exchanger. We raised the K^+ concentration by 10-fold (from 2 to 20 mM) to test whether the K^+–Cl^- transporter contributes to CO_2/HCO_3^--dependent ^{14}C-MA accumulation. Raising the K^+ concentration produced negligible effect ($P > 0.05$; $n = 4$; Fig. 2*B*), implying that the K^+–Cl^- cotransporter is unlikely to be involved. In parallel experiments with sister plates, cells were treated with the assay solution that contained $NMDG^+$ instead of Na^+. Replacing Na^+ caused a small reduction (Fig. 2*C*). Adding the NHE blocker dimethylamiloride (0.1 mM) had negligible effect on this reduction (data not shown).

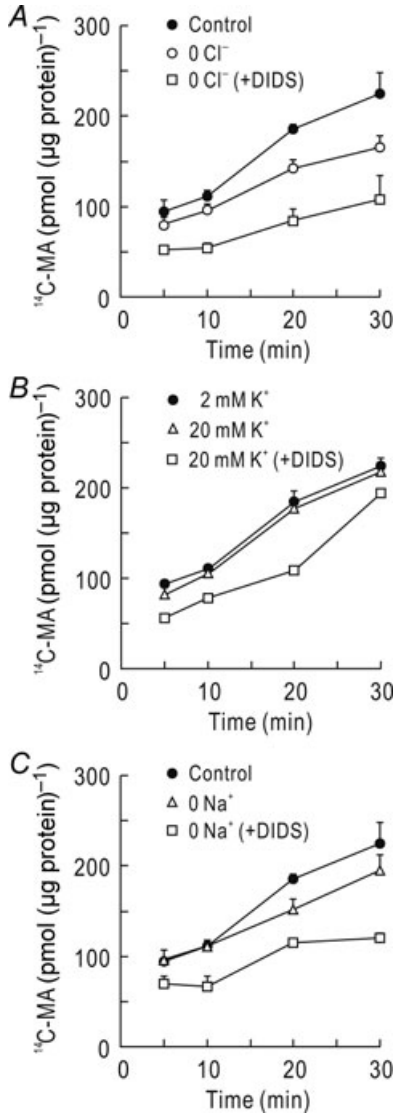

Figure 2. Effects of Cl^- and Na^+ replacement and K^+ concentration on ^{14}C-MA accumulation
All assay solutions contained 5% CO_2, 33 mM HCO_3^- (pH 7.4). *A*, effect of Cl^- replacement. The Cl^- in the ^{14}C-MA assay solution was replaced by gluconate in the absence or presence of 0.5 mM DIDS ($n = 4$ for each). *B*, effect of raising K^+ concentration. The K^+ concentration in the assay solution was raised from 2 to 20 mM ($n = 4$). *C*, effect of Na^+ replacement. The Na^+ in the assay solution was replaced by $NMDG^+$ ($n = 4$).

Acid-loading HCO_3^- extrusion is found in ST-1 cells

We monitored pH_i changes from an alkali load using the pH-sensitive fluorescent dye, BCECF. Upon the application of 20 mM NH_4Cl in CO_2/HCO_3^--free solution (Fig. 3*A*), pH_i was rapidly increased and then nearly reached a plateau ($n = 5$). Lack of intracellular acidification reflects inhibition of carrier-mediated CH_3-NH_3^+ transport by bumetanide and ouabain in our experiments. The recovery was slightly enhanced by DIDS, the nature of which is unclear. Thus, DIDS had negligible effect on pH_i alone. In the presence of 5% CO_2, 33 mM HCO_3^- (Fig. 3*B*), however, the pH_i recovery towards the resting pH was significantly faster (dpH_i/dt of $-27.8 \pm \times 10^{-4}$ pH units s^{-1}; $n = 5$), indicating acid-loading HCO_3^- transport in the cells. This acid-loading process was substantially reduced by DIDS (-6.9×10^{-4} pH units s^{-1}; $P < 0.05$). Figure 3*C* summarizes the pH_i recovery rates from an alkali load in the absence and presence of CO_2/HCO_3^-. The dpH_i/dt in the presence of CO_2/HCO_3^- was higher and inhibited by DIDS (75%).

DIDS-sensitive ^{14}C-MA accumulation is abolished at low pH_i

Figure 4*A* shows ^{14}C-MA accumulation rates measured in the absence and presence of 5% CO_2, 33 mM HCO_3^- (pH 7.4). The measurements without DIDS (open columns in the figure) revealed that the accumulation rate was higher in the presence of CO_2/HCO_3^- (2.5 ± 0.4 pmol μg^{-1} min^{-1} in Hepes *versus* 6.1 ± 0.4 pmol μg^{-1} min^{-1} in CO_2/HCO_3^-; $n = 3$ for each; the unit is pmoles of ^{14}C-MA per microgram of total protein per minute), corresponding to a 2.4-fold increase ($n = 0.001$; *a* in Fig. 4*A*). Adding 0.5 mM DIDS to the assay solution had negligible effect in the absence of CO_2/HCO_3^-, but reduced the accumulation (4.5 ± 0.1 pmol μg^{-1} min^{-1}; $n = 3$; $P = 0.002$; *c* in Fig. 4*A*). The remaining value after

subtracting the value in Hepes represents the DIDS-insensitive accumulation ($P = 0.01$; *d* in Fig. 4*A*).

We then incubated cells at pH 7.4 and 6.8 (adjusted with $NaHCO_3$ in 5% CO_2) for 24 h and measured ^{14}C-MA accumulation in the presence of 5% CO_2, 33 mM HCO_3^- (pH 7.4; Fig. 4*B*). Acidic incubation at pH 6.8–6.9 has been used for the *in vitro* study of metabolic acidosis in other systems (O'Hayre *et al.* 2006; Tsuruoka *et al.* 2006). Adding 0.5 mM DIDS to the assay solution reduced ^{14}C-MA accumulation in control cells ($P = 0.007$; $n = 5$; *a* in Fig. 4*B*). However, DIDS showed negligible inhibition in cells incubated at pH 6.8. The ^{14}C-MA accumulation was similar in the two groups of cells treated and untreated with DIDS ($P > 0.05$; *b* in Fig. 4*B*), indicating that DIDS-sensitive HCO_3^- transport was inactivated after acidic incubation. This inactivation caused a substantial decrease in the accumulation.

Figure 4*C* shows mean steady-state pH_i in the presence of CO_2/HCO_3^- determined using the ratiometric pH-sensitive dye, BCECF-AM. The steady-state pH_i in cells incubated at pH 6.8 was 6.96 ± 0.03 ($n = 4$), significantly lower than 7.28 ± 0.04 ($n = 4$) for control cells ($P = 0.001$). Thus, acidic incubation lowered steady-state pH_i. Incubating cells at pH 6.8 for 24 h caused 20% cell death compared with 8% for control conditions, determined by Trypan Blue staining (data not shown). The unhealthy or dead cells are swollen, exhibit blebbing and are morphologically distinguishable from healthy cells. We used healthy cells for pH measurements.

NBCn1 in the MTAL cells is upregulated by acidic incubation

The above data show that the ^{14}C-MA accumulation after acidic incubation is lower than that in control incubation conditions, when compared in the absence of DIDS. This is probably due to inactivation of DIDS-insensitive HCO_3^- extruders at low pH_i, but it is also possible that acid-extruding HCO_3^- loaders are stimulated in acidic conditions and reduce the conversion of CH_3-NH_3 to CH_3-NH_3^+. To test whether NBCn1 protein expression is affected, we incubated cells at pH 6.8 for 24 h and performed immunoblotting using the anti-NBCn1 antibody (Cooper *et al.* 2009). Control cells were incubated at pH 7.4 for 24 h.

Figure 5*A* shows a representative immunoblot analysis of membrane preparations from cells at 0 h and after acidic incubation for 24 h. An immunoreactive band of 135 kDa was detected. A band of 250 kDa, which is a

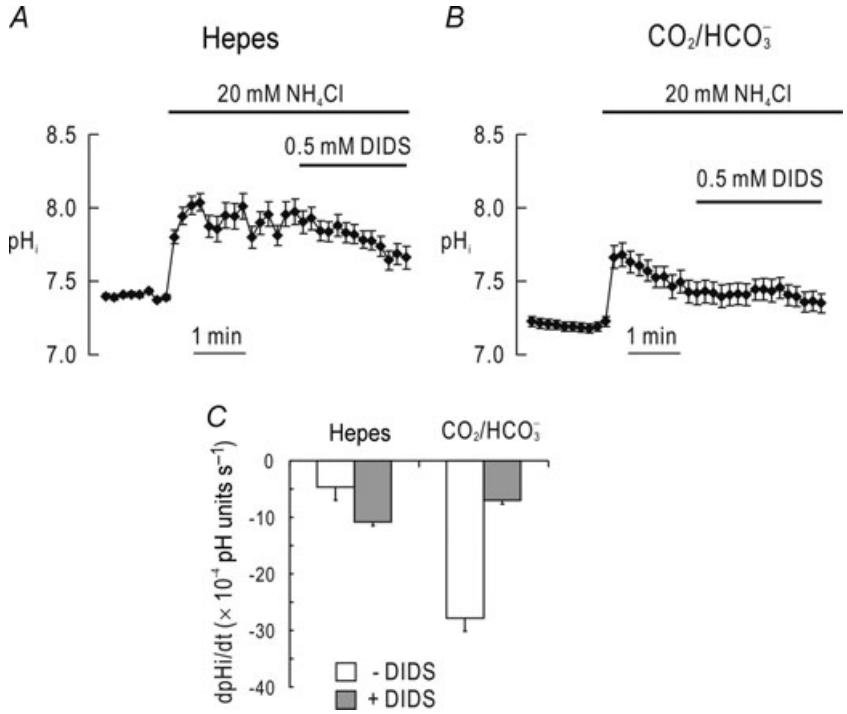

Figure 3. The CO_2/HCO_3^--induced stimulation of the pH_i recovery from an alkali load
A, pH_i recovery from an alkali load in the absence of CO_2/HCO_3^-. Cells were treated with 20 mM NH_4Cl, and 0.5 mM DIDS was applied during the pH_i recovery from an alkali load ($n = 5$). *B*, pH_i recovery from an alkali load in the presence of 5% CO_2, 33 mM HCO_3^-. Cells were subjected to the protocol as described in *A* except that the experiment was done in the presence of CO_2/HCO_3^- ($n = 5$). *C*, summary of the pH_i recovery rate. Data were obtained from the experiments in *A* and *B*.

multimeric form of the protein as shown in neurons (Cooper *et al.* 2009), was additionally recognized. The detection of this higher molecular weight band varies depending upon experiments (H. S. Yang, unpublished observation). Expression of NBCn1 was increased after acidic incubation. Analysed by quantitative measurements of NBCn1 relative to β-actin (Fig. 5*B*), the increase was 48% ($P = 0.04$; $n = 3$). The upregulation was progressively larger with longer incubation periods (Fig. 5*C* and *D*); thus, at 72 h, the NBCn1 expression level after acidic incubation was nearly threefold higher than for control conditions. We also performed immunoblotting of cells that were incubated in the medium containing 10 mM NH_4Cl (pH 7.4) for 24 h and found a marked upregulation of NBCn1 after NH_4Cl treatment (Fig. 5*E* and *F*). This result indicates that the pH in the media is not responsible for upregulating the transporter.

In other experiments, the blot was probed with the anti-AE2 antibody (Frische *et al.* 2004) to determine whether acidic incubation affects the Cl^-–HCO_3^- exchanger. An immunoreactive band of 110 kDa was recognized but remained unaffected after acidic incubation (Fig. 6*A*). The molecular weight of AE2 in ST-1 cells was smaller than ~150 kDa in the kidney (Frische *et al.* 2004). Quantitative measurements of AE2 relative to β-actin revealed negligible difference between control and acidic incubation ($P > 0.05$; $n = 4$; Fig. 6*B*). We also performed immunoblotting with antibodies to AE1 and AE3 but did not find immunoreactive bands (data not shown).

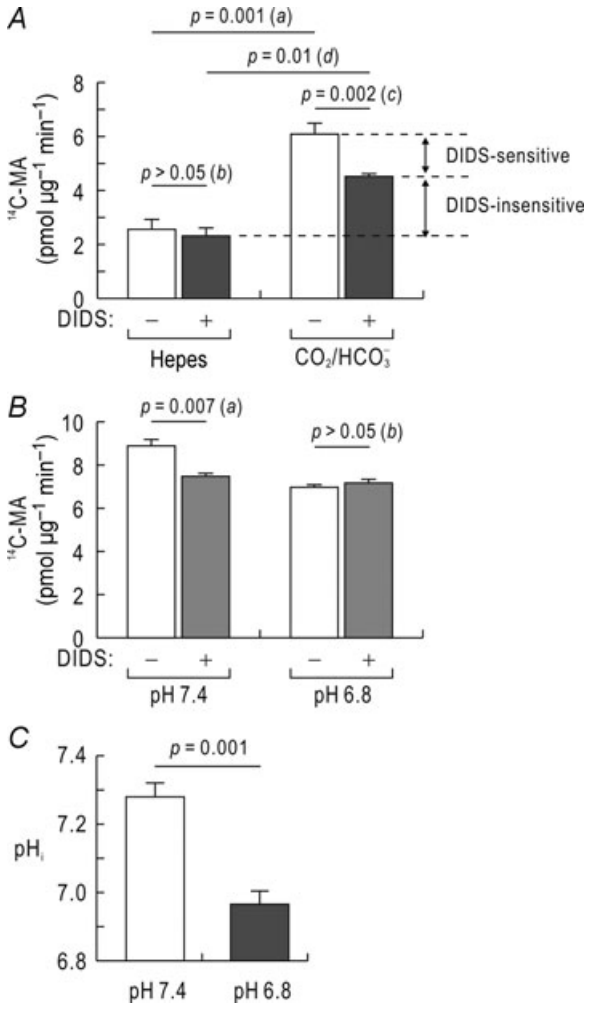

Figure 4. Accumulation of ^{14}C-MA in cells after acidic incubation
A, effect of DIDS on ^{14}C-MA accumulation. Cells were treated with ^{14}C-MA assay solution in the absence and presence of 5% CO_2, 33 mM HCO_3^- (pH 7.4) for 30 min. The concentration of DIDS was 0.5 mM. The *P* values for comparison (*a*–*d*) are described in the text. Data were averaged from three experiments. *B*, effect of acidic pH_i on ^{14}C-MA accumulation. Cells were incubated in the medium of pH 7.4 or 6.8 for 24 h. Experiments were done by treating cells with CO_2/HCO_3^--buffered ^{14}C-MA assay solution (pH 7.4) for 20 min. Data were averaged from five experiments. *C*, steady-state pH_i. Cells were incubated in the medium of pH 7.4 or 6.8 for 24 h, and their pH_i was measured in CO_2/HCO_3^- at the corresponding pH ($n = 4$ for each). The measurements were done using the ratiometric pH-sensitive dye BCECF-AM.

NBCn1 expressed in *Xenopus* oocytes increases ^{14}C-MA accumulation

The above results led us to postulate that the HCO_3^- loader, NBCn1, might contribute to NH_4^+/NH_3 uptake particularly in acidic conditions, in which the transporter is upregulated. To test this hypothesis, we expressed the rat renal NBCn1-E splice variant (Yang *et al.* 2009) in *Xenopus* oocytes and measured ^{14}C-MA accumulation. Oocyte membranes are very impermeable to NH_3 (Burckhardt & Frömter, 1992; Nakhoul *et al.* 2001), indicating that oocytes can preferentially trap NH_3, contrary to our ST-1 cell system. For ^{14}C-MA accumulation experiments with oocytes, therefore, bumetanide and ouabain were not added to the assay solution. In CO_2/HCO_3^--free ND96 solution (Fig. 7*A*), oocytes expressing NBCn1-E and control oocytes accumulated ^{14}C-MA in a similar manner ($P > 0.05$; $n = 16$ oocytes for each). However, in a solution buffered with 5% CO_2, 25 mM HCO_3^- (Fig. 7*B*), oocytes expressing NBCn1-E showed a significant increase in ^{14}C-MA accumulation ($P < 0.05$; $n = 16$ for each; two-way ANOVA with Bonferroni *post hoc* test). The difference between the two groups of oocytes was already substantial 10 min after exposure to CO_2/HCO_3^- and continued thereafter. Figure 7*C* shows CO_2/HCO_3^--dependent ^{14}C-MA accumulation calculated by subtracting values in CO_2/HCO_3^--free solution from values in CO_2/HCO_3^- solution. A profound increase was produced in oocytes expressing NBCn1-E. Replacement of Na^+ abolished the difference in the accumulation (Fig. 7*D*).

We then performed two-electrode voltage clamp to test whether NBCn1-E produces currents by NH_4^+. Determined before and 1 min after applying 20 mM NH_4Cl, current–voltage relationships showed negligible

change (Fig. 8*A* and *B*). The slope conductances were similar before and after NH_4Cl application ($P > 0.05$ for both control and NBCn1-E; $n = 6$ for control and $n = 8$ for NBCn1-E; Fig. 8*C*). Oocytes expressing NBCn1-E had more positive zero-current voltage and higher slope conductance due to the ionic conductance intrinsic to NBCn1 (Choi *et al.* 2000; Cooper *et al.* 2005).

Discussion

The major findings of the present study are as follows: (1) CO_2/HCO_3^- enhances ^{14}C-MA accumulation in the non-polarized MTAL cells, and this effect is inhibited by DIDS; (2) CO_2/HCO_3^--dependent ^{14}C-MA accumulation is affected by replacing Cl^-; (3) at low pH_i, CO_2/HCO_3^--dependent ^{14}C-MA accumulation is not inhibited by DIDS; (4) NBCn1, but not AE2, in ST-1 cells is upregulated in acidic conditions; and (5) NBCn1 in *Xenopus* oocytes stimulates CO_2/HCO_3^--dependent ^{14}C-MA transport. These findings are important for understanding the effect of HCO_3^- transporters on NH_4^+/NH_3 uptake in the MTAL and provide evidence that cells regulate NH_4^+/NH_3 uptake by altering the expression and activity of NBCn1 and AE2 in response to acid–base disturbance. A cell model for the effect of HCO_3^- transporters on NH_4^+/NH_3 uptake in ST-1 cells is described in Fig. S1.

We used radiolabelled MA to analyse the effect of HCO_3^- transporters on NH_4^+/NH_3 uptake. Methylammonium/methylammonia (pK of 10.3) has been extensively used as an NH_4^+/NH_3 surrogate in many studies (Soupene *et al.* 2002; Westhoff *et al.* 2002;

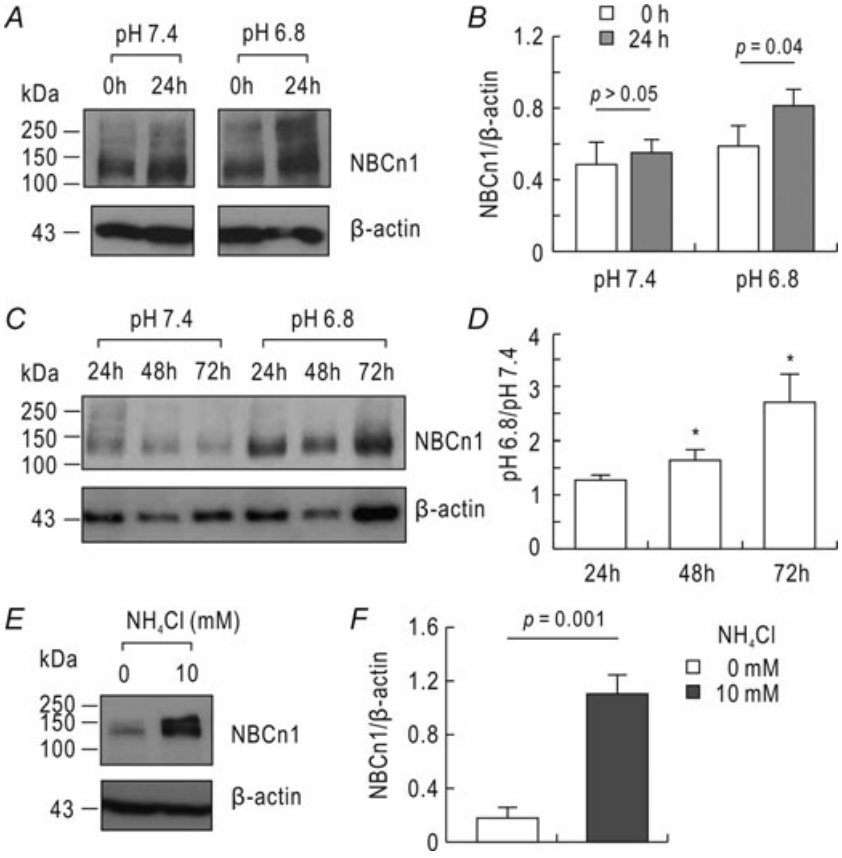

Figure 5. Effect of acidic incubation on NBCn1 expression
A, immunoblot for NBCn1. Cells were incubated in the medium of pH 7.4 *versus* 6.8 for 0 or 24 h. Plasma membranes were isolated and subjected to immunoblotting with the anti-NBCn1 antibody. The blots were striped and reprobed with the β-actin antibody. One of three experiments is shown. *B*, quantitative measurements of NBCn1. The pixel intensity of NBCn1 was measured and normalized to β-actin ($n = 3$). The P value less than 0.05 was considered significant. *C*, immunoblot for NBCn1 at normal and acidic incubation for 24, 48 and 72 h. One of three experiments is shown. *D*, quantitative measurements of NBCn1. The value of NBCn1/β-actin at pH 6.8 is presented relative to the value at pH 7.4 at each time point. The data were analysed by one-way ANOVA with Bonferroni *post hoc* test; $^*P < 0.05$. *E*, NBCn1 expression in cells treated with NH_4Cl. Cells were incubated in the medium (pH 7.4) containing 0 or 10 mM NH_4Cl for 24 h. The NaCl was replaced by NH_4Cl. One of three experiments is shown. *F*, quantitative measurements of NBCn1.

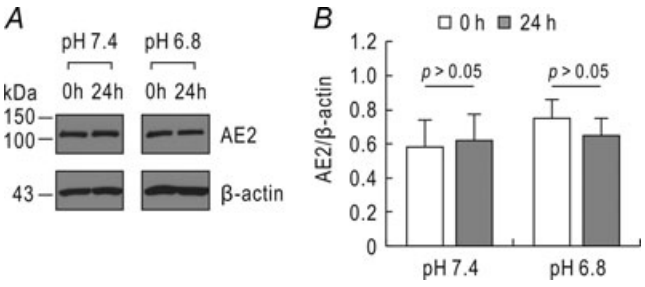

Figure 6. Effect of acidic incubation on AE2 expression
A, immunoblot for AE2. The experimental procedure was similar to that in Fig. 5 except that the blot was probed with the anti-AE2 antibody. One of four experiments is shown. *B*, quantitative measurements of AE2. The pixel intensity of AE2 was measured and normalized to β-actin.

Verlander *et al.* 2003). When a cell is exposed to CH_3-NH_3^+/CH_3-NH_2, membrane-permeable CH_3-NH_2 rapidly enters the cell and associates with H^+ to form CH_3-NH_3^+. The reaction then reaches a plateau as CH_3-NH_2 becomes equilibrated inside and outside the cell. During this plateau phase, charged CH_3-NH_3^+ is slowly transported into the cytosol via carrier proteins and then dissociates into CH_3-NH_2 and H^+. If carrier-mediated CH_3-NH_3^+ entry is inhibited, the total intracellular CH_3-NH_3^+/CH_3-NH_2 (i.e. MA) is primarily determined by the amount of intracellular H^+ supplied for the conversion of CH_3-NH_2 to CH_3-NH_3^+. A high level of intracellular H^+ supply increases the conversion and accumulates more ^{14}C-MA, whereas a low level of intracellular H^+ supply decreases it. Therefore, the magnitude of ^{14}C-MA accumulation in our experiments reflects the activity of acid–base transporters in the cell.

In analysing the effect of HCO_3^- transporters on NH_4^+/NH_3 uptake, we found that DIDS reduces ^{14}C-MA accumulation (Figs 1, 2, and 4). Additional experiments with Cl^- replacement showed the Cl^-–HCO_3^- exchanger influencing ^{14}C-MA accumulation. In CO_2/HCO_3^- solution, CO_2 enters the cell and produces H^+ and HCO_3^-. By moving HCO_3^- out of the cell, the Cl^-–HCO_3^- exchanger concomitantly provides intracellular H^+ available for the conversion of CH_3-NH_2 to CH_3-NH_3^+. Nonetheless, our data suggest that the Cl^-–HCO_3^- exchanger would not be the major HCO_3^- extruder affecting NH_4^+/NH_3 uptake in ST-1 cells because Cl^- replacement partly inhibits ^{14}C-MA accumulation. In combination with Cl^- replacement, DIDS produced more

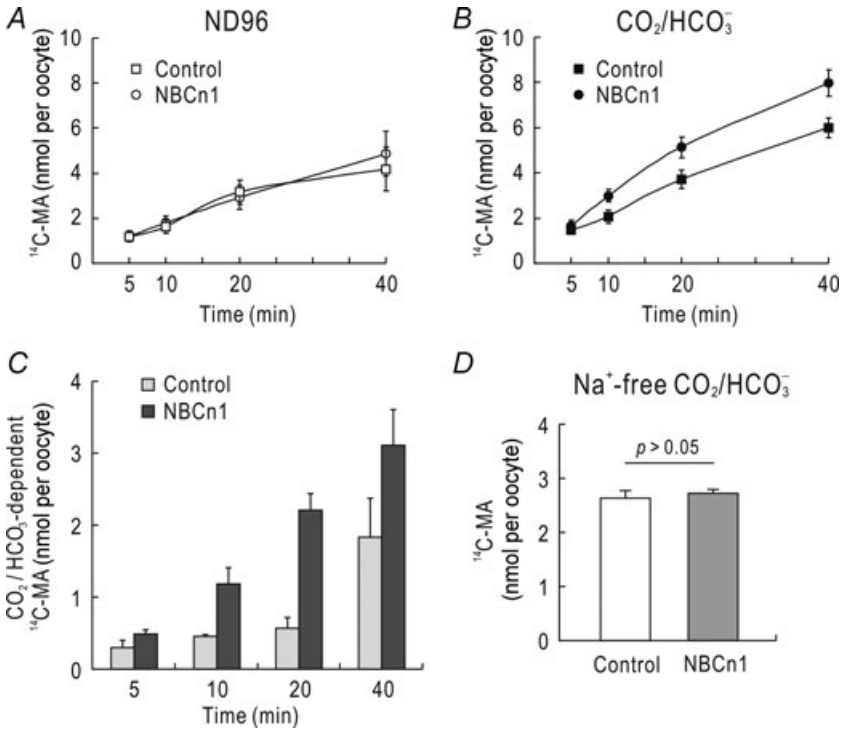

Figure 7. Time course of ^{14}C-MA accumulation in *Xenopus* oocytes expressing NBCn1
A and *B*, ^{14}C-MA accumulation in oocytes injected with water or NBCn1-E cRNA. Oocytes were incubated with the ^{14}C-MA assay solution (no bumetanide and ouabain) in the absence (*A*) or presence of CO_2/HCO_3^- (*B*; pH 7.4), and then rapidly washed with ice-cold unlabelled MA solution at different time points. The accumulation is expressed as nmoles per oocyte. Data were averaged from four independent experiments with a total of 16 oocytes per group. *C*, CO_2/HCO_3^--dependent ^{14}C-MA accumulation. The accumulation was calculated by subtracting values in CO_2/HCO_3^--free ND96 solution from values in CO_2/HCO_3^--containing solution in *A* and *B*. *D*, effect of Na^+ replacement on ^{14}C-MA accumulation. The Na^+ was replaced with $NMDG^+$ ($n = 3$ for each).

severe inhibition than Cl^- replacement alone (Fig. 2*A*), implying that there is an additional DIDS-sensitive HCO_3^--extruding process. This HCO_3^- extrusion does not require K^+, because raising the K^+ concentration by 10-fold had no effect on ^{14}C-MA accumulation (Fig. 2*B* and *C*). Likewise, it also does not require Na^+, because replacing Na^+ had only a small effect. The molecular nature of this HCO_3^- extrusion is unclear.

In acidic conditions, the activity of Cl^-–HCO_3^- exchange appears to be minimal because DIDS had no significant effect on ^{14}C-MA accumulation after acidic incubation (Fig. 3). Stewart *et al.* (2001) reported that AE2 is inactivated at low pH_i. The AE2-mediated $^{36}Cl^-$ uptake in *Xenopus* oocytes is almost abolished when the oocyte pH_i is at 6.88. Furthermore, AE2 expression remained unaffected after acidic incubation (Fig. 6). This lack of AE2 upregulation is comparable to the previous report (Quentin *et al.* 2004) that AE2 in the MTAL of the kidney is not upregulated by chronic metabolic acidosis. Together with the lack of DIDS inhibition and the negligible change in AE2 expression, our data support the idea of Cl^-–HCO_3^- exchange being inactivated at low pH_i.

In contrast to AE2, that NBCn1 in ST-1 cells was upregulated after acidic incubation (Fig. 5). This is in good agreement with the reports (Kwon *et al.* 2002; Odgaard *et al.* 2004) that NBCn1 expression and activity in rat MTAL are enhanced during chronic metabolic acidosis induced by NH_4Cl feeding. It is also comparable to our recent report (Cooper *et al.* 2009) that NBCn1 in primary cultures of rat hippocampal neurons is upregulated after incubation at pH 6.2–6.5 for 1 h. Others have reported that NBCn1 in rat MTAL is unaffected or downregulated during chronic metabolic acidosis induced by obstruction of the ureter (Wang *et al.* 2008) and calcineurin inhibition (Mohebbi *et al.* 2009). The reason for the disparity among several reports remains unclear, but we think that the severity and duration of acidosis may determine the onset of NBCn1 upregulation. NBCn1 normally moves HCO_3^- into the cell and extrudes acids, implying that its upregulation compensates excessive H^+ load caused by acidification (Kwon *et al.* 2002; Odgaard *et al.* 2004). Consistent with this, we observed NBCn1 upregulation after incubating ST-1 cells with NH_4Cl (Fig. 5*E*), further supporting the importance of pH_i for NBCn1 upregulation.

In *Xenopus* oocytes, NBCn1 increased CO_2/HCO_3^--dependent ^{14}C-MA accumulation (Fig. 7). Oocyte membranes are less permeable to NH_3 than to NH_4^+ (Burckhardt & Frömter, 1992; Nakhoul *et al.* 2001), similar to the apical membrane of the MTAL (Kikeri *et al.* 1989). Oocytes expressing NBCn1 showed a relatively slow change in pH_i upon NH_4Cl application compared with control oocytes (see Fig. S2). We think that the increased accumulation of ^{14}C-MA in NBCn1-expressing oocytes reflects the increased carrier-mediated NH_4^+ transport in these oocytes. It has been documented that NH_4Cl induces a slow acidification with depolarization of oocyte membranes. However, our data in Fig. 8 show no measurable changes in currents and membrane potential during NH_4Cl application. The reason for this disparity is unclear, although we note that NH_4Cl-induced voltage changes in oocytes have been measured in CO_2/HCO_3^--free solutions. It is also interesting to note that NH_4^+ transport in oocytes may be inhibited by acidic pH_i (Boldt *et al.* 2003). Regardless, our data provide evidence that NBCn1 enhances NH_4^+ transport as determined by ^{14}C-MA accumulation. This might be important for regulating NH_4^+ transport in the MTAL, particularly during chronic metabolic acidosis.

In summary, our data provide *in vitro* evidence for NBCn1 upregulation in acidic environments. The upregulation may provide a constant supply of HCO_3^-

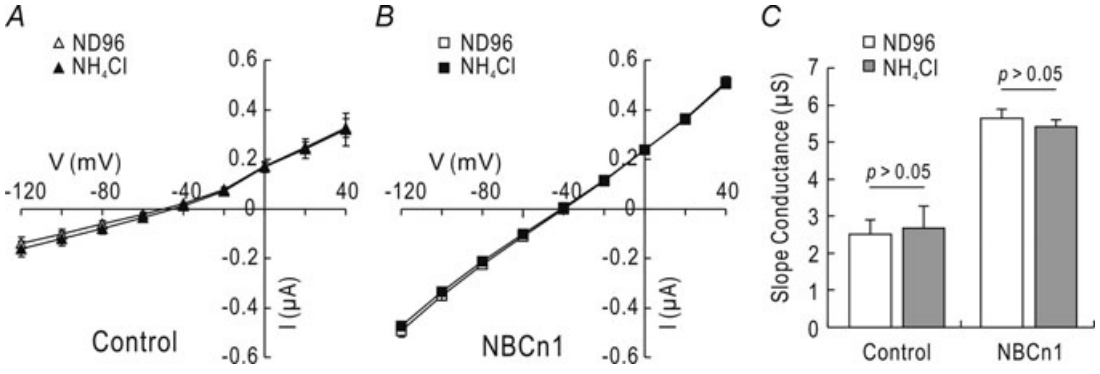

Figure 8. Two-electrode voltage clamp of oocytes
A and *B*, current–voltage relationships for currents before and after NH_4Cl application. Oocytes were clamped at −60 mV, and voltage commands from −120 to +40 mV were applied. Recordings were made in CO_2/HCO_3^--free ND96 solution and 1 min after switching to a solution containing 20 mM NH_4Cl. Data were averaged from six controls and eight NBCn1-E-expressing oocytes. *C*, slope conductance. The conductance was computed near the zero-current potential in *A* and *B*.

to the cell and enhance NH_4^+/NH_3 uptake by buffering the intracellular H^+ load. It will be interesting to examine a possible NH_4^+/NH_3 movement via NBCn1 in future experiments.

References

Boldt M, Burckhardt G & Burckhardt BC (2003). NH_4^+ conductance in *Xenopus laevis* oocytes. III. Effect of NH_3. *Pflügers Arch* **446**, 652–657.

Bourgeois S, Masse S, Paillard M & Houillier P (2002). Basolateral membrane Cl^-, Na^+, and K^+coupled base transport mechanisms in rat MTALH. *Am J Physiol Renal Physiol* **282**, F655–F668.

Brosius FC, Nguyen K, Stuart-Tilley AK, Haller C, Briggs JP & Alper SL (1995). Regional and segmental localization of AE2 anion exchanger mRNA and protein in rat kidney. *Am J Physiol* **269**, F461–F468.

Burckhardt BC & Frömter E (1992). Pathways of NH_3/NH_4^+ permeation across *Xenopus laevis* oocyte cell membrane. *Pflügers Arch* **420**, 83–86.

Chang MH, Dipiero J, Sonnichsen FD & Romero MF (2008). Entry to "HCO_3^- tunnel" revealed by SLC4A4 human mutation and structural model. *J Biol Chem* **283**, 18402–18410.

Choi I, Aalkjaer C, Boulpaep EL & Boron WF (2000). An electroneutral sodium/bicarbonate cotransporter NBCn1 and associated sodium channel. *Nature* **405**, 571–575.

Cooper DS, Saxena NC, Yang HS, Lee HJ, Moring AG, Lee A & Choi I (2005). Molecular and functional characterization of the electroneutral Na/HCO_3 cotransporter NBCn1 in rat hippocampal neurons. *J Biol Chem* **280**, 17823–17830.

Cooper DS, Yang HS, He P, Kim E, Rajbhandari I, Yun CC & Choi I (2009). Sodium/bicarbonate cotransporter NBCn1/slc4a7 increases cytotoxicity in magnesium depletion in primary cultures of hippocampal neurons. *Eur J Neurosci* **29**, 437–446.

Frische S, Zolotarev AS, Kim YH, Praetorius J, Alper S, Nielsen S & Wall SM (2004). AE2 isoforms in rat kidney: immunohistochemical localization and regulation in response to chronic NH4Cl loading. *Am J Physiol Renal Physiol* **286**, F1163–F1170.

Gamba G & Friedman PA (2009). Thick ascending limb: the Na^+:K^+:2Cl^- co-transporter, NKCC2, and the calcium-sensing receptor, CaSR. *Pflugers Arch* **458**, 61–76.

Good DW (1994). Ammonium transport by the thick ascending limb of Henle's loop. *Annu Rev Physiol* **56**, 623–647.

Good DW & Watts BA III (1996). Functional roles of apical membrane Na^+/H^+ exchange in rat medullary thick ascending limb. *Am J Physiol Renal Physiol* **270**, F691–F699.

Kaplan JH (2002). Biochemistry of Na,K-ATPase. *Annu Rev Biochem* **71**, 511–535.

Kikeri D, Azar S, Sun A, Zeidel ML & Hebert SC (1990). Na^+-H^+ antiporter and Na^+-(HCO_3^-)n symporter regulate intracellular pH in mouse medullary thick limbs of Henle. *Am J Physiol Renal Physiol* **258**, F445–F456.

Kikeri D, Sun A, Zeidel ML & Hebert SC (1989). Cell membranes impermeable to NH_3. *Nature* **339**, 478–480.

Kinne R, Kinne-Saffran E, Schutz H & Scholermann B (1986). Ammonium transport in medullary thick ascending limb of rabbit kidney: involvement of the Na^+,K^+,Cl^- cotransporter. *J Membr Biol* **94**, 279–284.

Kone BC & Higham S (1999). Nitric oxide inhibits transcription of the Na^+-K^+-ATPase α1-subunit gene in an MTAL cell line. *Am J Physiol Renal Physiol* **276**, F614–F621.

Kone BC, Schwobel J, Turner P, Mohaupt MG & Cangro CB (1995). Role of NF-κB in the regulation of inducible nitric oxide synthase in an MTAL cell line. *Am J Physiol Renal Physiol* **269**, F718–F729.

Kraut JA & Kurtz I (2005). Metabolic acidosis of CKD: diagnosis, clinical characteristics, and treatment. *Am J Kidney Dis* **45**, 978–993.

Kwon TH, Fulton C, Wang W, Kurtz I, Frokiaer J, Aalkjaer C & Nielsen S (2002). Chronic metabolic acidosis upregulates rat kidney Na-HCO_3 cotransporters NBCn1 and NBC3 but not NBC1. *Am J Physiol Renal Physiol* **282**, F341–F351.

Liu Z, Chen Y, Mo R, Hui C, Cheng JF, Mohandas N & Huang CH (2000). Characterization of human RhCG and mouse Rhcg as novel nonerythroid Rh glycoprotein homologues predominantly expressed in kidney and testis. *J Biol Chem* **275**, 25641–25651.

Liu Z, Peng J, Mo R, Hui C & Huang CH (2001). Rh type B glycoprotein is a new member of the Rh superfamily and a putative ammonia transporter in mammals. *J Biol Chem* **276**, 1424–1433.

Marini AM, Matassi G, Raynal V, Andre B, Cartron JP & Cherif-Zahar B (2000). The human Rhesus-associated RhAG protein and a kidney homologue promote ammonium transport in yeast. *Nat Genet* **26**, 341–344.

Mohebbi N, Mihailova M & Wagner CA (2009). The Calcineurin inhibitor FK506 (tacrolimus) is associated with transient metabolic acidosis and altered expression of renal acid-base transport. *Am J Physiol Renal Physiol* **297**, F499–F509.

Nakhoul NL, Hering-Smith KS, Abdulnour-Nakhoul SM & Hamm LL (2001). Ammonium interaction with the epithelial sodium channel. *Am J Physiol Renal Physiol* **281**, F493–F502.

Odgaard E, Jakobsen JK, Frische S, Praetorius J, Nielsen S, Aalkjaer C & Leipziger J (2004). Basolateral Na^+-dependent HCO_3^- transporter NBCn1-mediated HCO_3^- influx in rat medullary thick ascending limb. *J Physiol* **555**, 205–218.

O'Hayre M, Taylor L, Andratsch M, Feifel E, Gstraunthaler G & Curthoys NP (2006). Effects of constitutively active and dominant negative MAPK kinase (MKK) 3 and MKK6 on the pH-responsive increase in phosphoenolpyruvate carboxykinase mRNA. *J Biol Chem* **281**, 2982–2988.

Park HJ, Rajbhandari I, Yang HS, Lee S, Cucoranu D, Cooper DS, Klein JD, Sands JM & Choi I (2010). Neuronal expression of sodium/bicarbonate cotransporter NBCn1 (SLC4A7) and its response to chronic metabolic acidosis. *Am J Physiol Cell Physiol* **298**, C1018–C1028.

Quentin F, Eladari D, Frische S, Cambillau M, Nielsen S, Alper SL, Paillard M & Chambrey R (2004). Regulation of the Cl^-/HCO_3^- exchanger AE2 in rat thick ascending limb of Henle's loop in response to acid-base and sodium balance. *J Am Soc Nephrol* **15**, 2988–2997.

Soupene E, Lee H & Kustu S (2002). Ammonium/methylammonium transport (Amt) proteins facilitate diffusion of NH_3 bidirectionally. *Proc Natl Acad Sci U S A* **99**, 3926–3931.

Stewart AK, Chernova MN, Kunes YZ & Alper SL (2001). Regulation of AE2 anion exchanger by intracellular pH: critical regions of the NH_2-terminal cytoplasmic domain. *Am J Physiol Cell Physiol* **281**, C1344–C1354.

Sun AM (1998). Expression of Cl^-/HCO_3^- in the basolateral membrane of mouse medullary thick ascending limb. *Am J Physiol Renal Physiol* **274**, F358–F364.

Tsuruoka S, Watanabe S, Purkerson JM, Fujimura A & Schwartz GJ (2006). Endothelin and nitric oxide mediate adaptation of the cortical collecting duct to metabolic acidosis. *Am J Physiol Renal Physiol* **291**, F866–F873.

Verlander JW, Miller RT, Frank AE, Royaux IE, Kim YH & Weiner ID (2003). Localization of the ammonium transporter proteins RhBG and RhCG in mouse kidney. *Am J Physiol Renal Physiol* **284**, F323–F337.

Vorum H, Kwon TH, Fulton C, Simonsen B, Choi I, Boron W, Maunsbach AB, Nielsen S & Aalkjaer C (2000). Immunolocalization of electroneutral Na-HCO_3^- cotransporter in rat kidney. *Am J Physiol Renal Physiol* **279**, F901–F909.

Wagner CA (2007). Metabolic acidosis: new insights from mouse models. *Curr Opin Nephrol Hypertens* **16**, 471–476.

Wang G, Li C, Kim SW, Ring T, Wen J, Djurhuus JC, Wang W, Nielsen S & Frokiaer J (2008). Ureter obstruction alters expression of renal acid-base transport proteins in rat kidney. *Am J Physiol Renal Physiol* **295**, F497–F506.

Weiner ID & Hamm LL (2007). Molecular mechanisms of renal ammonia transport. *Annu Rev Physiol* **69**, 317–340.

Westhoff CM, Ferreri-Jacobia M, Mak DO & Foskett JK (2002). Identification of the erythrocyte Rh blood group glycoprotein as a mammalian ammonium transporter. *J Biol Chem* **277**, 12499–12502.

Xu J, Wang Z, Barone S, Petrovic M, Amlal H, Conforti L, Petrovic S & Soleimani M (2003). Expression of the Na^+-HCO_3^- cotransporter NBC4 in rat kidney and characterization of a novel NBC4 variant. *Am J Physiol Renal Physiol* **284**, F41–F50.

Yang HS, Cooper DS, Rajbhandari I, Park HJ, Lee S & Choi I (2009). Inhibition of rat Na^+–HCO_3^- cotransporter (NBCn1) function and expression by the alternative splice domain. *Exp Physiol* **94**, 1114–1123.

Acknowledgements

The work was supported by the NIH grant R01-GM078502 and NS046653 (M.B.), National Kidney Foundation, and Emory URC grant (I.C,). Soojung Lee was supported by a Korea Research Foundation grant funded by the Korean Government (KRF-2007-357-C00121).

Author's present address

H. J. Lee: Department of Radiology and Radiological Sciences, Vanderbilt University, MCN CCC-1121, 1161 21st Avenue South, Nashville, TN 37232, USA.

Supporting Information

Online supplemental material for this paper can be accessed at:

http://jp.physoc.org/cgi/content/full/jphysiol.2008.165084/DC1

As a service to our authors and readers, this journal provides supporting information supplied by the authors. Such materials are peer-reviewed and may be re-organized for online delivery, but are not copy-edited or typeset. Technical support issues arising from supporting information (other than missing files) should be addressed to the authors.